Available online at www.sciencedirect.com
ScienceDirect
Remote Sensing of Environment 107 (2007) 200–210
Remote Sensing of Environment
www.elsevier.com/locate/rse

Comparison of MISR and MODIS cloud-top heights in the presence of cloud overlap

C.M. Naud [a,*], B.A. Baum [b,1], M. Pavolonis [c], A. Heidinger [c], R. Frey [d], H. Zhang [d]

[a] *Department Applied Physics and Applied Mathematics, Columbia University/GISS, 2880 Broadway, New York, NY 10025, United States*
[b] *NASA Langley Research Center, Hampton, VA, United States*
[c] *NOAA/NESDIS, United States*
[d] *CIMSS, University of Wisconsin–Madison, Madison, WI 53706, United States*

Received 1 February 2006; received in revised form 31 July 2006; accepted 3 September 2006

Abstract

Coincident MISR and MODIS cloud-top heights retrieved above two vertically pointing radar sites (ARM-SGP and UK-CFARR) are compared for 54 scenes between March 2000 and October 2003. The difference between MODIS and MISR cloud-top heights is assessed in situations where multiple cloud layers are present in a vertical column (i.e., cloud overlap or multilayered cloud). MISR stereo cloud-top heights are known to be sensitive to low-level clouds of high contrast (between two camera views) even if high clouds with a wide range of optical thicknesses are also present in the scene. MODIS retrieved cloud-top heights do not experience this problem as long as the highest cloud layer has a visible optical thickness greater than approximately 1. Consequently, the difference in cloud-top heights between MODIS and MISR is often large and positive in cloud overlap conditions. In cloud overlap conditions, small differences between MODIS and MISR cloud-top heights can be found where both instruments detect the highest cloud layer or, on the contrary, where they both fail to detect the highest cloud but instead detect some lower level cloud. The comparison with radar cloud-top heights on a 21-scene subset confirmed that large differences are associated with cloud overlap, but also showed that small differences can be found in similar situations if the highest layer is of large contrast (both instruments detect the highest cloud layer) or of extremely small optical thickness (both instruments fail to detect the highest cloud layer). With the use of a cloud-typing technique applied to MODIS data that can also identify areas containing cloud overlap, small differences were found to occur for 60–70% of all overlap pixels examined here, highlighting the weakness of using the MODIS-MISR cloud-top height differences as a sole indicator for automated cloud overlap detection. While the accuracy of the MODIS cloud-top pressure/height algorithm decreases as the cirrus optical thickness becomes less than 1, the MISR approach may still be able to infer an accurate cloud-top height depending on the cloud contrast between two view angles. However, synergy between the difference in MODIS-MISR cloud-top height analysis and the MODIS cloud-typing method could improve overlap detection for thin cirrus over low cloud situations and provide additional information on the cloud-top height of two distinct layers.
© 2006 Elsevier Inc. All rights reserved.

Keywords: Cloud; Overlap; MISR; MODIS; Cloud-top height; Cloud type

1. Introduction

Operational satellite retrievals of cloud properties currently rely on the assumption that only one cloud layer exists in any particular field of view. Satellite-based retrieval methods are not sensitive to multilayered clouds for the case in which the uppermost cloud is optically thick. However, retrieval errors increase as the opacity of the uppermost cloud decreases, such as for the situation of an optically thin ice cloud overlying lower-level water clouds. Surface based observations (Hahn et al., 1982, 1984) indicate the presence of low-level clouds in about half of the cases where cirrus could be observed. It is thus important to be able to automatically identify cloud overlap

* Corresponding author. Tel.: +1 212 678 5572; fax: +1 212 678 5552.
E-mail address: cnaud@giss.nasa.gov (C.M. Naud).
[1] Current affiliation is: Space Science and Engineering Center, University of Wisconsin–Madison, Madison, WI 53706, United States.

0034-4257/$ - see front matter © 2006 Elsevier Inc. All rights reserved.
doi:10.1016/j.rse.2006.09.030

situations and monitor them from space. Methods have been proposed that exploit differing visible and infrared spectral signatures unique to cloud overlap (e.g. Baum & Spinhirne, 2000; Baum et al., 1995, 2003; Chang & Li, 2005; Nasiri & Baum, 2004; Pavolonis & Heidinger, 2004). These methods are restricted to situations when thin cirrus overlies a low-level water cloud and are thus limited by the optical thickness of the highest cloud layer. Others also use ground-based microwave instruments (Huang et al., 2005).

Our goal is to investigate the retrieved cloud-top heights obtained by two different sensors on the same NASA Terra platform: the Multiangle Imaging SpectroRadiometer (MISR, Diner et al., 1998) and the MODerate resolution Imaging Spectroradiometer (MODIS, Salomonson et al., 1989). Our focus is on cases in which two cloud layers are present in the column (called multilayered cloud or cloud overlap), in particular when thin cirrus overlies a lower-level water cloud. Each instrument provides a different view of the cloud structure, and by understanding the strength of each retrieval approach, our eventual goal is to improve multilayered cloud retrieval using a data fusion approach. Naud et al. (2002) found that because the MISR retrieval method is tuned to the layer of higher contrast, MISR stereo heights often, but not always, refer to lower cloud layers even if higher and optically thinner cloud layers are present in the field of view. MODIS cloud-top pressures and temperatures are produced operationally using the CO_2-slicing method (e.g. Menzel et al., 1983) and can be converted to cloud-top heights using reanalysis profiles of temperature. This method was found to be relatively insensitive to multilayer cloud situations (Naud et al., 2005a), although in the extreme case of very thin clouds (visible optical thickness less than 1), the highest cirrus layers may not be detected if thicker cloud layers are present below (Naud et al., 2005b).

In this study, cloud-top heights (CTH) are obtained from both instruments and differences in cloud-top heights between MODIS and MISR are calculated. Theoretically, a large positive difference (MODIS-MISR) should be the indication that MISR stereo heights are detecting a low-level cloud layer of large contrast when MODIS cloud-top heights refer to a high-level cloud layer. This method provides a straightforward indication of multilayered clouds and provides some insight as to the tendencies of each retrieval approach. To assess the reliability of each approach, both MISR and MODIS cloud-top heights are compared to those provided by a ground-based vertically pointing millimeter wave radar at two sites: the ARM Southern Great Plains site in the USA (SGP) and the Chilbolton Facility for Atmospheric and Radio Research in the UK (CFARR). In addition, a routine that detects cloud type and overlap was applied to MODIS radiances (Pavolonis & Heidinger, 2004; Pavolonis et al., 2005).

The instruments and corresponding cloud data are described in Section 2. Section 3 shows the comparison between radar and MODIS and MISR cloud-top heights when cloud overlap is detected with the radar, and Section 4 examines the difference MODIS- MISR cloud-top height as a function of cloud type. Conclusions are given in Section 5.

2. Data description

2.1. MISR stereo cloud-top heights

MISR is a push-broom camera instrument that measures 0.45, 0.56, 0.68 and 0.87 μm radiances at 9 different along-track view angles with 4 forward, one nadir and 4 aft cameras (0°, ±26.1°, ±45.6°, ±60°, ±70.5°). Its nominal resolution is 275 m (250 m for nadir) and its swath width is 380 km. The narrow swath means that the global coverage is obtained every 9 days. Cloud-top heights are inferred with a stereo technique that uses the 0.87 μm channel at nadir and ±26.1° (Moroney et al., 2002).

The MISR stereo height algorithm first infers the cloud-top winds, then corrects for wind advection displacement in one of the views to match with the other view, and then infers the stereo heights (Moroney et al., 2002). These stereo heights are named "best winds". The stereo heights are retrieved for all 1.1 km pixels in the scene, regardless of the cloud content of the pixel. When the stereo height retrieval fails, the radiometric cloud mask and an independent measure of surface height and type is automatically used to fill in the gaps with the surface height. The theoretical accuracy is estimated to be 562 m (Moroney et al., 2002) and MISR stereo heights were found to be in agreement with surface heights within 1 km for clear-sky scenes where wind advection is not an issue (Muller et al., 2002).

If the wind retrieval fails, the stereo heights are still retrieved but placed in a different field called "without winds". For this study, we decided to use the "without winds" stereo heights when the "best winds" stereo heights were unavailable to increase the number of comparison cases. We found that for most pixels with both retrievals available, the mean wind correction was within 1 km which is the accuracy expected for the "best winds" MISR cloud-top heights (Marchand et al., in press; Naud et al., 2005a). In addition, it is necessary to test each stereo height with respect to the surface altitude given in the geolocation information file. When the stereo height is less than the surface height plus 562 m, the pixel is flagged as clear-sky. Stereo heights tend to contain "blunders" or anomalously high heights. These "blunders" can be defined as isolated anomalously large heights compared to the heights found in the surrounding pixels. Research into how to automatically eliminate these blunders is still ongoing and apart from a 20 km cut-off, pixels containing anomalously high cloud-top heights are not automatically removed in the operational product (Moroney, 2006, private communication). To mitigate the impact of anomalously high cloud-top heights, a threshold was imposed of 13 km at Chilbolton and 15 km at SGP, based on the average tropopause height at these locations. The application of these thresholds removed less than 1% of all pixels per scene on average. MODIS cloud-top heights are available at 5 km resolution (Menzel et al., 2002) and the latitude–longitude grids for both instruments are not aligned. Consequently it was necessary to reproject the MISR cloud-top heights onto the same latitude–longitude grid as the MODIS cloud-top heights. We chose to keep the median MISR cloud-top height for cloudy pixels within a 0.02° radius area centered on each MODIS grid point. This process helps filter out any remaining blunders.

2.2. MODIS cloud-top heights

MODIS is an imager that measures radiances in 36 spectral bands from 0.4 to 14.2 μm, with nadir spatial resolutions from 250 m to 1 km depending on the wavelength. With a swath width of 2330 km, global coverage can be obtained in approximately 2 days. MODIS cloud-top heights are specifically calculated with the latest algorithm used for MODIS collection 5 (MODIS data are currently being reprocessed from the beginning of the mission using improved algorithms and the new version is called collection 5). Cloud-top pressures and temperatures are normally provided in the product, but cloud-top heights have to be obtained from use of independent ancillary profiles. For this study cloud-top heights are calculated directly using geopotential height profiles from the same ancillary dataset as used operationally with the cloud-top pressure algorithm.

The CO_2-slicing method (e.g. Menzel et al., 1983) makes use of differential atmospheric CO_2 absorption in two adjacent MODIS bands (13.3/13.6 μm, 13.6/13.9 μm, 13.9/14.2 μm) to simultaneously retrieve cloud-top pressure and cloud effective emissivity (defined as cloud fraction multiplied by cloud emissivity; Menzel et al., 2002). Although the algorithm was initially designed for 4 pairs, the 11 μm/13.3 μm pair was dismissed due to differences in cloud emissivity between the two channels. The emissivity is less of an issue for ice clouds than it is for water clouds. Cloud phase information is not employed yet in the CO_2-slicing algorithm. Retrievals are performed for 5 × 5 arrays of 1-km pixels. Ratios of difference between clear and cloudy-sky radiances are compared to forward radiance calculations based on gridded 1°-resolution numerical weather prediction (NWP) model output temperature and moisture profiles. The corresponding cloud-top pressure is kept that minimizes the error between modeled and computed radiances for the CO_2 channels. Because upwelling radiances in these bands are primarily sensitive to the middle and upper troposphere, the algorithm is most useful for retrieval of clouds at these levels, including transmissive cirrus. For clouds below about 700 hPa, the "window channel" method is used: measured 11-μm brightness temperatures are compared to modeled values for opaque clouds at various atmospheric levels to find the level that minimizes the difference between observed and calculated values. Once the cloud-top pressures are obtained the reanalysis profiles of geopotential heights are used for the conversion into cloud-top heights. Collection 5 reprocessing uses an updated forward radiance model, as well as changes in the averaging method over the 5 × 5 pixel areas. For Collection 5, only observed cloudy radiances are compared to modeled clear-sky values, rather than clear and cloudy observed radiances together. This has little effect on middle and high cloud retrievals where clouds are mostly large in areal extent (cloud fraction is 100% over 25 km^2), but does lead to somewhat higher retrieved cloud-top heights and colder cloud-top temperatures in the case of broken low-level clouds. A complete description of the improvements to the algorithm used in collection 5 is available on the MODIS web site.

2.3. MODIS cloud type

Pavolonis and Heidinger (2004) have developed an automated method to detect multilayered clouds from satellite imagery, for the Advanced Very High Resolution Radiometer (AVHRR) and the Visible Infrared Imager Radiometer Suite (VIIRS). In addition to multilayered cloud detection, Pavolonis et al. (2005) present AVHRR and VIIRS algorithms that further classify cloudy satellite pixels into various categories. Since the VIIRS will have similar spectral channels as the MODIS, the VIIRS cloud-typing algorithm was developed and tested extensively on MODIS data. Using the combined methodology described in Pavolonis and Heidinger (2004) and Pavolonis et al. (2005), clouds observed from satellite can be classified into one of the following categories: *warm liquid water clouds*, *supercooled water/mixed phase clouds*, *opaque ice clouds*, *cirrus clouds*, and *multilayered clouds*. The warm liquid water category includes clouds that are composed of liquid water droplets that have an infrared radiative temperature greater than 273.16 K (given by the measured 11-μm brightness temperature). The second class accounts for clouds that are either composed entirely of supercooled water droplets or both ice and supercooled water (e.g. liquid water is detected but the 11-μm brightness temperature < 273.16 K). Opaque ice clouds are considered to be non-transmissive or weakly-transmissive in the infrared (i.e. with a visible optical thickness > 5) that are either entirely composed of ice crystals or opaque clouds that have glaciated tops consistent with deep convection. The fourth cloud type consists of single layer ice clouds that are transmissive. Most cirrus clouds fall into this category. Last, the multilayered category identifies situations in which more than one cloud layer is present in the field of view. All classifications are determined through a series of physically based spectral tests. See Pavolonis et al. (2005) for a detailed description of the cloud-typing algorithm and a validation of the methodology.

For the analysis presented in this paper, the multilayered cloud detection is of particular interest so a brief algorithm summary will be given here. See Pavolonis and Heidinger (2004) and Heidinger and Pavolonis (2005) for a much more detailed discussion and validation. The Pavolonis and Heidinger multilayered cloud detection algorithm was designed to detect the presence of cirrus clouds overlapping a lower liquid water cloud using channels in the 0.65, 1.38, 1.65, 11, and 12-μm regions of the spectrum. The algorithm most effectively detects cloud overlap when an ice cloud of visible optical thickness between 0.5 and 4.0 overlaps a liquid water cloud with a visible optical thickness > 5. The algorithm generally does not detect overlapping water clouds (e.g. liquid water over liquid water) or overlapping ice clouds (e.g. ice over ice). In spite of these limitations, validation studies (Pavolonis & Heidinger, 2004) and global analysis (Heidinger & Pavolonis, 2005) show that the Pavolonis and Heidinger algorithm captures a large subset of the multilayered cloud. Heidinger and Pavolonis (2005) show that roughly 40% of all ice clouds overlap water clouds. These results are consistent with microwave/infrared derived multilayered cloud amounts (Ho et al., 2003) and surface observations (Hahn & Warren, 2002).

Table 1
Summary of comparison between MISR, MODIS and radar cloud-top heights for 21 scenes over SGP and CFARR

	Date and location	Situation	MISR CTH (km)	MODIS CTH (km)	Radar low CTH (km)	Radar high CTH (km)	Cloud type (% of pixels in ±0.2° box) as determined from MODIS data				
							Water	Mixed phase	Opaque ice	Cirrus	Cloud overlap
A1	2000-10-07, CFARR	Overlap detected by radar and cloud-typing but MISR indicates lowest cloud layer while MODIS indicates highest	4.6±0.6	6.0±0.4	3.1±0.7	6.8±0.1	0.0	21.3	0.0	0.0	78.7
A2	2000-11-23, SGP		3.5±2.8	7.0±0.9	4.3±0.8	9.3±0.0	0.0	0.1	2.7	0.3	96.9
A3	2001-03-15, SGP		3.4±2.2	7.0±1.1	3.3±0.7	8.0±0.1	0.0	8.1	12.5	1.9	77.5
A4	2003-05-08, CFARR		1.1±1.1	10.0±2.9	3.4±3.9	12.6±0.0	13.0	0.0	0.0	43.8	40.4
A5	2003-05-18, CFARR		3.5±2.0	6.0±1.1	3.0±0.4	9.6±0.8	0.0	4.2	12.2	1.1	82.5
B1	2001-12-12, SGP	Overlap detected by radar and cloud-typing but MISR indicates highest cloud layer with MODIS	6.9±0.4	5.0±0.9	2.0±0.0	6.8±2.1	2.3	16.6	3.8	3.6	73.7
B2	2001-12-29, CFARR		8.7±0.9	8.0±1.1	1.8±0.3	8.3±0.4	0.0	0.0	2.6	26.6	70.9
B3	2002-03-16, SGP		9.9±2.2	10.0±0.3	5.4±0.4	10.9±0.1	0.0	0.0	2.9	0.0	97.1
B4	2002-06-04, SGP		9.7±4.4	11.0±1.5	2.5±0.0	12.3±0.3	1.3	0.5	14.6	15.5	68.0
B5	2003-03-05, SGP		8.5±2.9	9.0±1.3	1.6±0.0	9.9±0.1	0.0	3.1	10.1	1.4	85.4
C1	2001-02-27, SGP	3 cloud layers, MODIS and MISR indicate middle layer (lowest layer from radar not indicated here)	4.2±0.9	5.0±0.9	5.6±0.5	9.7±0.1	0.0	4.9	0.0	0.2	94.9
C2	2001-11-08, SGP		5.2±1.1	6.0±1.4	6.0±0.2	10.4±0.0	7.6	12.0	6.8	35.3	36.1
C3	2002-01-29, SGP		8.4±1.9	8.0±1.2	8.8±0.1	11.9±0.2	0.0	0.1	5.1	0.1	93.8
D1	2001-02-18, SGP	2 high-cloud layers, but MISR and MODIS indicate lowest cloud layer	7.6±2.0	6.0±1.8	7.7±1.8	12.0±0.0	6.8	12.0	0.0	75.3	3.1
D2	2003-05-31, SGP	2 high cloud layers, but MISR and MODIS indicate highest cloud layer	9.0±3.0	10.0±1.0	7.6±1.1	12.4±0.0	0.3	0.1	0.0	85.9	13.7
D3	2003-05-27, CFARR	Two low-level cloud layers MODIS CTH close to highest and MISR CTH close to lowest	1.2±0.4	2.0±0.5	1.5±0.1	3.0±0.2	93.0	6.4	0.0	0.0	0.6
E1	2001-04-01, CFARR	Overlap but highest layer not over radar at the time of the overpass	1.0±0.3	7.0±0.8	1.0±0.1	1.0±3.9	0.0	4.3	0.0	0.7	94.9
E2	2001-06-06, CFARR	Overlap but lowest layer not over radar at the time of the overpass	2.4±0.5	6.0±0.6	7.2±0.2	7.2±0.1	1.2	23.8	0.3	4.3	70.4
E3	2002-10-12, SGP	Highest layer broken so MODIS cloud-top height and cloud-typing not matching radar very well	3.2±1.7	6.0±1.8	2.9±0.1	11.2±0.0	76.5	4.5	0.7	2.2	16.1
E4	2002-08-16, SGP	Lowest cloud broken so MODIS cloud-type not matching radar very well	1.7±2.1	11.0±0.7	1.8±0.0	13.7±0.1	0.0	0.0	0.0	62.3	37.7
E5	2002-01-30, CFARR	Cloud-top height of the highest layer vary rapidly so not match between MODIS cloud-top height and radar sampled around overpass time	7.6±1.4	8.0±0.2	2.7±0.0	5.1±3.0	0.0	0.0	0.0	0.0	100

The MISR and MODIS cloud-top heights correspond to the median in a ±0.2° box centered on the radar, while the radar cloud-top heights correspond to the median during the 40-min period.

The multilayered cloud detection algorithm is most prone to false detection when single layer ice clouds reside over surfaces that are bright in the near-infrared such as dry vegetation or deserts. Throughout the rest of this paper the MODIS cloud-typing algorithm (including the multilayered cloud detection) will be referred to as the PH0405 algorithm.

The 1-km resolution cloud type product is sampled to match the 5 km resolution of MODIS cloud-top heights by using the cloud-type of the central pixel in the 5×5 km areas. The frequency of occurrence of each cloud-type in ±0.2° boxes centered on the radar site for each date was estimated using the 1 km product and compared to the 5 km product. The differences were negligible for all dates selected here.

2.4. Millimeter wave cloud radars

Chilbolton 94-GHz millimeter wave cloud radar data were processed with a similar algorithm as the SGP 35-GHz radar

data (Clothiaux et al., 2000). The two radars have different wavelengths and receivers, making the SGP radar more sensitive to thin high clouds (Mace et al., 2005) but also more sensitive to low altitude clutter in summer (usually insects and vegetation debris) that can be confused with low-level cloud detection. The algorithm uses information from a nearby lidar to decide if a low-level layer of hydrometeors is likely embedded in the clutter. The data processing algorithm produces a cloud mask that indicates clear, cloudy, clutter, mixture of hydrometeor and clutter or bad data. The mask is provided every 10 s and every 60 m at CFARR and 45 m at SGP. On the days when the radar site is located within the narrow MISR swath, the cloud-top heights of the highest and lowest layer detected above the radar are sampled over a 5-minute period from MODIS acquisition start time, and for 10, 20 and 40 min centered on MODIS start-time. The median cloud-top height is then estimated for each time period and cloud layer. Two methods are used to decide if a case could be kept. If the median cloud-top heights of the highest cloud layer do not depart radically from each other when comparing the 4 time periods (cloud-top heights not varying by more than 3 km per layer) and two distinct cloud layers are present for a significant period of time close to the TERRA overpass, the case is selected for comparison. In parallel, if more than one cloud layer is present for at least half of the time in the 40-minute accumulated cloud mask, the case is also kept. The radar cloud-top heights used for the comparison are those obtained with the median value of data sampled over a 40 min time period.

3. Comparison of MISR-MODIS difference in cloud-top height and radar

Over the period of the TERRA mission (March 2000 to present), 21 dates were selected between March 2000 and October 2003 for which (a) the MISR narrow swath encompassed the radar site (250 dates at CFARR and 252 at SGP), (b) the radar was functioning (203 dates at SGP and 111 at CFARR), (c) the radar detected clouds (130 dates at SGP and 86 at CFARR), and (d) both MODIS and MISR cloud-top retrievals were available. This gave a total of 39 dates. A final quality check was performed by visual inspection of the radar cloud mask and MISR and MODIS cloud-top height maps to remove cases where single level clouds had not been properly filtered out or if broken cloud layers could lead to ambiguities. These conditions were met for 7 cases at CFARR and 14 at SGP. There were fewer cases at CFARR because the radar was under repair from March 2002 to April 2003. All 21 cases are listed in Table 1 in the same order as discussed below.

Table 1 indicates the date of the scene, the median MISR, MODIS and radar lowest and highest layer cloud-top height values and the percentage of pixels per cloud type in the ±0.2° latitude–longitude box.

For cases A1 to A5 in Table 1, the radar and the MODIS cloud-typing method indicate the presence of more than one cloud layer. MODIS cloud-top heights are close to the cloud-top height of the highest layer detected with the radar. However, MISR cloud-top heights are close to the top of the lowest layer detected by the radar. These cases show that the difference between MODIS and MISR cloud-top heights can provide an indication of cloud overlap.

For cases B1 to B5, the radar and the MODIS cloud-typing method also indicate the presence of more than one cloud layer. However, this time both MODIS and MISR cloud-top heights are close to the top of the highest layers. For these cases, the contrast of the highest cloud layer is large enough for MISR stereo heights to detect the highest cloud in the scene.

Cases C1 to C3 were found to contain three cloud layers on the radar cloud mask. The MODIS cloud-typing indicate the presence of cloud overlap even if the two layers that are most frequent are found at mid- and high-level. Both MODIS and MISR cloud-top heights are found close to the middle layer, which is found at or above 5 km, and both fail to detect the highest cloud layer.

Cases D1 to D3 show scenes where two cloud layers were detected with the radar cloud mask but are of the same nature (two high clouds presumably composed of ice particles for D1 and D2 or two low-level water clouds for D3). For these cases, the cloud-typing technique did not detect cloud overlap. Case D1 shows that MODIS and MISR cloud-top heights refer to the lowest cloud layer and case D2 show that they both refer to the highest cloud layer, so the difference in (MODIS-MISR) cloud-top height may not indicate overlap either. For case D3, the MODIS cloud-top height refers to the highest of the two water cloud layers while the MISR cloud-top height is closer to the lowest cloud layer. This example implies the possibility of detecting more than one cloud layer even if the two layers are of the same phase.

The final five cases E1–E5 show situations where it is more complicated to compare the satellite retrievals with the radar estimates. Cases E1 and E2 show that although the MODIS cloud-typing indicates a predominance of cloud overlap and the difference between MODIS and MISR cloud-top height corroborates this fact, the radar cloud-top heights only indicate one cloud layer at the time of the overpass. These cases were nevertheless kept as longer sampling periods show the presence of two distinct cloud layers with cloud-top heights in agreement with MODIS and MISR. Cases E3 and E4 show situations where the broken nature of one of the layers detected with the radar means that the cloud-typing method is predominantly detecting either water or ice. However, MODIS and MISR cloud-top heights seem to agree with the radar highest and lowest cloud-top heights respectively. For case E5, the cloud-top height of the highest cloud is detected at lower altitude with the radar than with MODIS and MISR. Because this case was found at CFARR, there is an indication that the radar signal is attenuated, but there was also high variability of the cloud-top height of the highest layer, so it is difficult to gain much insight from this particular example.

These case studies, although in limited number, reveal that the method of inferring the presence of thin cirrus overlying lower-level clouds by looking for a discrepancy between the MODIS and MISR CTHs seems to hold promise. However, we also find that there are cases where both instruments fail to detect the thin cirrus and others where both instruments detect

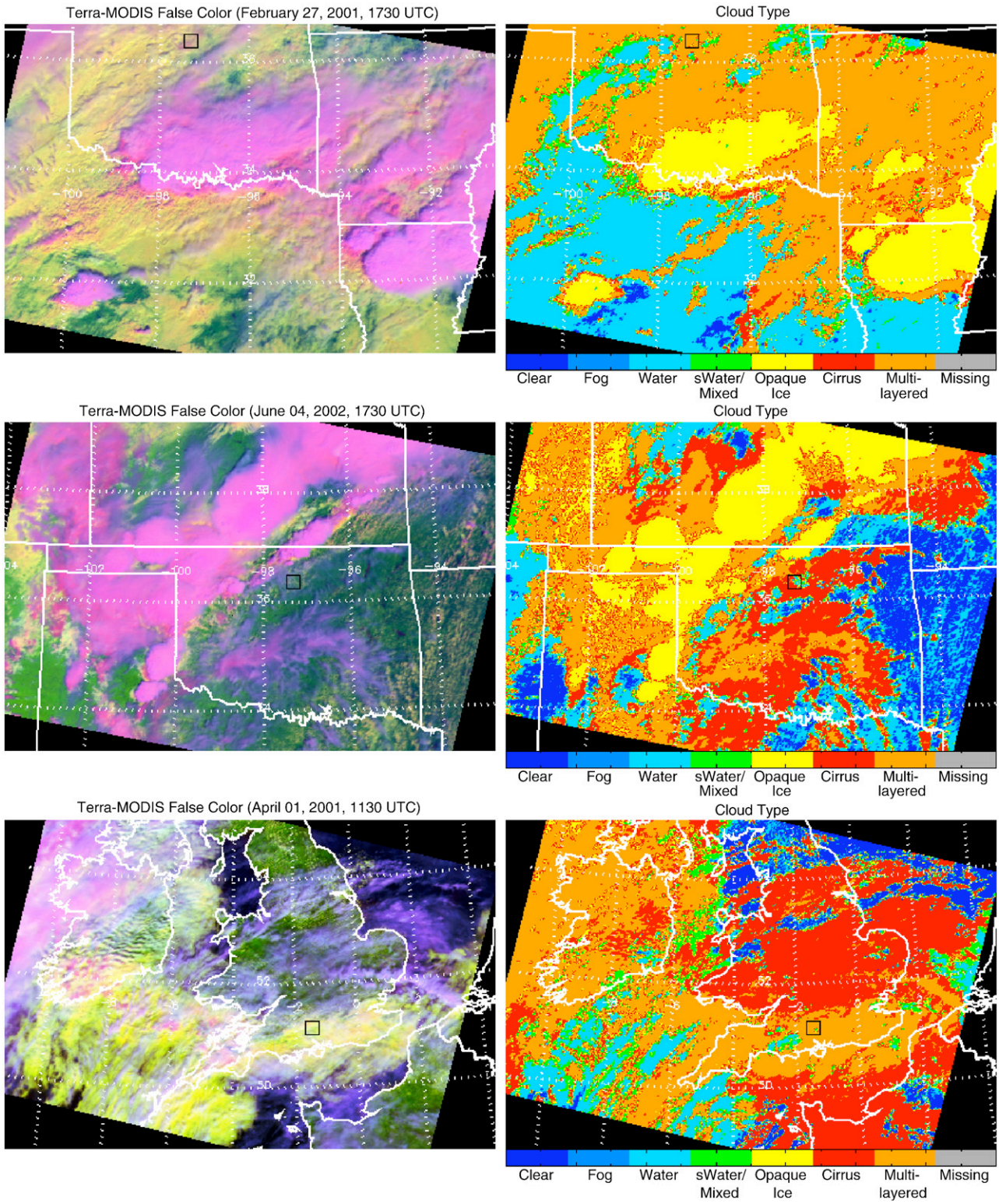

Fig. 1. Panel of MODIS false color images (left column) and MODIS cloud type (right column) for three different dates: top row shows 2001-02-27 at SGP for which MISR nor MODIS cloud-top heights identify the highest layer detected with the radar; middle row shows 2002-06-04 at SGP for which both MISR and MODIS cloud-top heights refer to the highest cloud layer; bottom row shows 2001-04-01 at CFARR for which MISR cloud-top heights refer to a lower cloud layer than MODIS cloud-top height. The center of the black square on each plot represents the radar site.

the high cloud so that nothing can be said about the low-level cloud. These are the two limiting situations, but at this stage we would at least need information on the optical thickness of the highest cloud layer to better characterize the MODIS-MISR limits. These could be obtained only if coincident downward-pointing lidar measurements were available and the highest

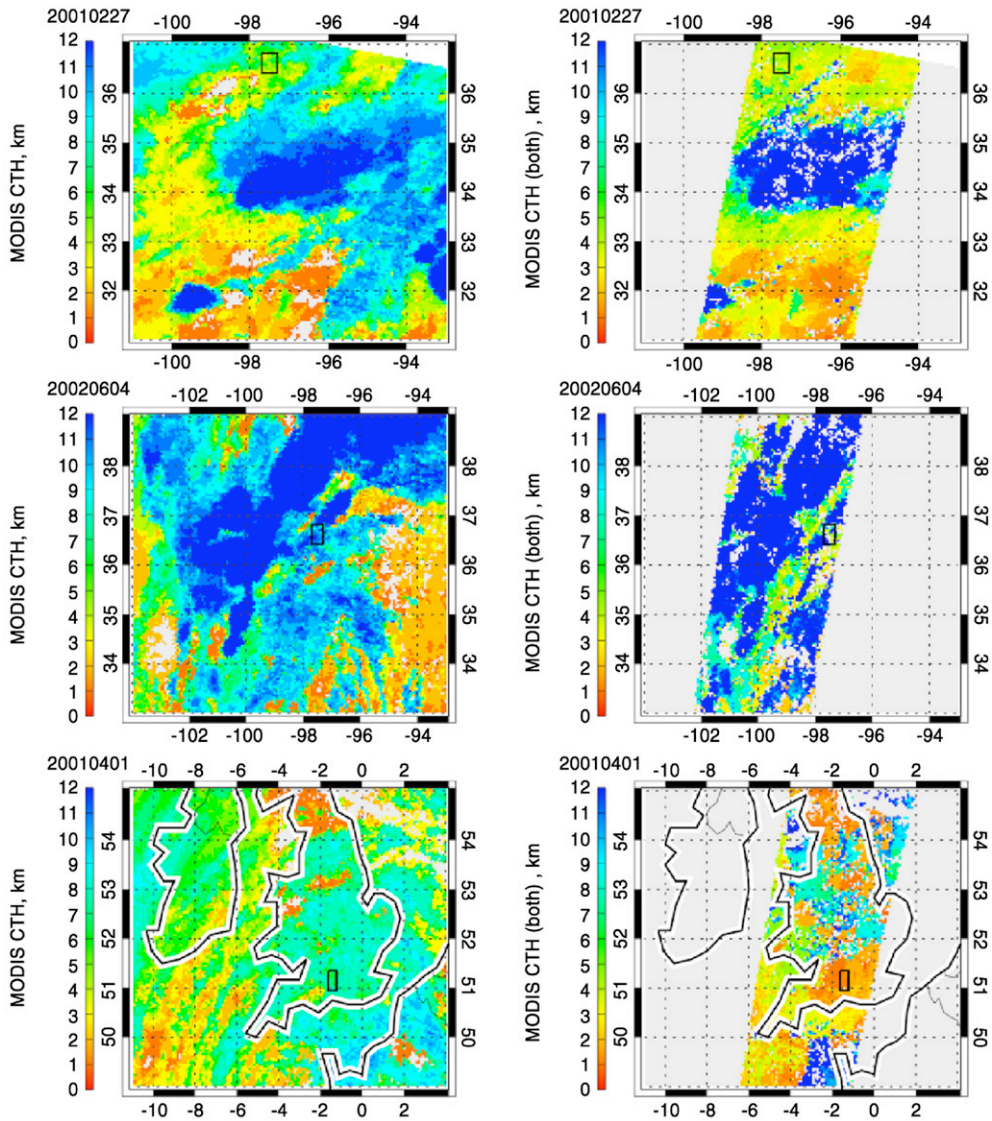

Fig. 2. Panel of MODIS (left column) and MISR (right column) cloud-top heights for the same three dates as on Fig. 1.

cloud was optically thin. Unfortunately, the limited sample of scenes prevents us from extracting meaningful statistics to assess the overall accuracy of this method. Another way of gaining insight is to use the MODIS cloud type algorithm results for all pixels within each scene that were selected over both sites (54 scenes in total, including scenes where the radar was not functioning or when single layer clouds were detected with the radar) and examine the distribution of MODIS-MISR cloud-top height differences as a function of cloud type. Another result that arises from these case studies is the possibility that the difference between MODIS and MISR cloud-top heights may also indicate cloud overlap even when both layers are composed of water clouds.

4. MISR-MODIS cloud-top height differences as a function of cloud type

The previous analyses focused only on a small portion of the data that encompassed either the SGP or CFARR sites. In this section, the entire area where MISR overlays MODIS is analyzed to increase the number of sampled points. At most, the region of interest will be as wide as the MISR swath (360 km) and as long as 2 concurrent MISR blocks, i.e. about 250 km. At SGP, 25 scenes were examined, while 29 were selected for CFARR. Special attention was given to areas in the scenes where large differences occurred between MODIS and MISR CTHs. All together, these scenes total nearly 300,000 cloudy pixels as points of comparison. For the area where the two imagers coincide, the distribution of the (MODIS-MISR) CTHs is calculated as a function of cloud type. To illustrate how the MODIS cloud type relates to the false color imagery and how it compares to MODIS and MISR cloud-top heights, we selected three dates at both sites and show the false color imagery and cloud-type in Fig. 1 and the corresponding MODIS and MISR cloud-top height maps in Fig. 2.

Fig. 3 shows the frequency of occurrence of the difference between MODIS and MISR cloud-top heights as a function of cloud type for each site separately. In addition, Table 2 shows

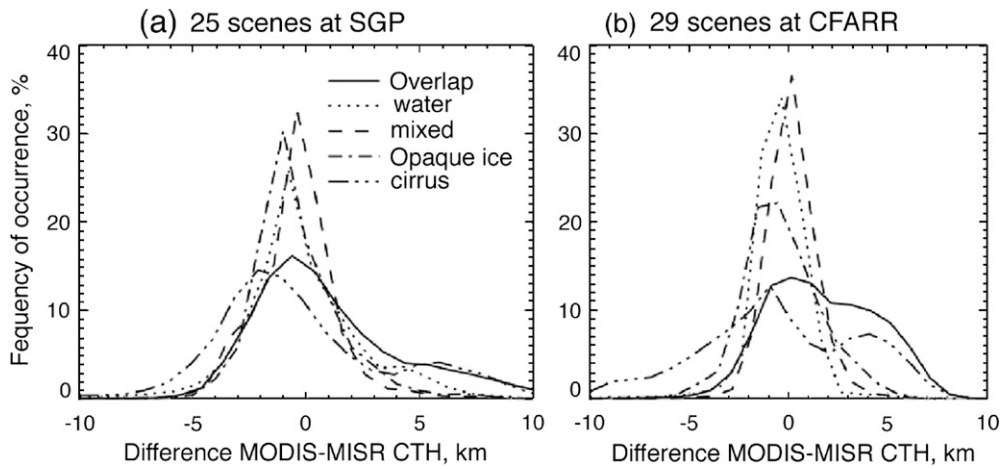

Fig. 3. Frequency of occurrence of difference between MODIS and MISR cloud-top heights as a function of cloud type at SGP (a) and CFARR (b): overlap (solid), water (dot line), mixed phase (dash line), opaque ice (dash–dot line), cirrus (dash–dot–dot–dot line), for all pixels per scene and 25 and 29 scenes respectively.

the percentage of pixels per cloud type for which either (1) MODIS and MISR cloud-top heights were above 5 km; (2) MODIS cloud-top heights were found above 5 km and MISR cloud-top heights below 5 km; (3) both MODIS and MISR cloud-top heights were found below 5 km and (4) MODIS cloud-top heights were found below 5 km while MISR cloud-top heights were found above 5 km. These percentages were calculated separately for SGP and CFARR.

4.1. Water clouds

The SGP frequency of occurrence plot (Fig. 3a) exhibits a peak for differences of −1 km, indicating a slight tendency for MISR cloud-top heights to be larger than MODIS cloud-top height. However, a secondary maximum can be noticed for differences around 4–5 km. Approximately 8% of the water pixels had an average MODIS cloud-top height of 7.5 km while the corresponding average MISR cloud-top heights were 2.67 km. Although 74% of all water pixels showed that both MODIS and MISR cloud-top heights were below 5 km, 8% of all water cases were found with both retrievals above 5 km. Another 10% of the water cloud pixels had MISR cloud-top heights greater than 5 km while MODIS cloud-top heights were below 5 km. In the latter situation, MISR cloud-top heights were found on average at 6.6 km and this overestimate could be explained by the presence of undetected blunders or a bad/no wind correction. These last two types of anomalies cause the average difference to be slightly negative. If we calculate the mean difference when both instrument retrievals concur that the clouds are below 5 km, MODIS cloud-top heights are found to be slightly larger by 350 m than MISR cloud-top heights. At CFARR, Fig. 3b shows the distribution of the CTH differences; only one peak is found at roughly null differences. At this site, 97% of all water cloud pixels were found with both MODIS and MISR retrievals below 5 km and the average difference was 0.1 ± 1.1 km. This result also reveals how the MODIS collection 5 cloud-top height retrievals have improved for low-level clouds compared to what was found in Collection 4 by Naud et al. (2005a). As far as MISR retrievals are concerned, less accurate stereo heights are expected at SGP due to generally stronger winds there compared to CFARR, causing more uncertainty for wind advection corrections.

Table 2
Percentage of pixels per cloud type with both MODIS and MISR CTH > 5 km, MODIS CTH > 5 km and MISR < 5 km, both MODIS and MISR < 5 km and MODIS CTH < 5 km and MISR CTH > 5 km for both sites

Cloud type	MODIS CTH > 5 km MISR CTH > 5 km		MODIS CTH > 5 km MISR CTH < 5 km		MODIS CTH < 5 km MISR CTH < 5 km		MODIS CTH < 5 km MISR CTH < 5 km	
	SGP (%)	CFARR (%)	SGP (%)	CFARR (%)	SGP (%)	CFARR (%)	SGP (%)	CFARR (%)
Water	8	0.5	8	0.5	74	97	10	2
Mixed	13	2	4	2	65	93	19	3
Opaque ice	84	70	8	13	5	12	3	5
Cirrus	67	30	21	23	6	28	6	19
Overlap	61	30	26	40	8	27	5	3

4.2. Mixed phase clouds

Mixed phase clouds (according to the MODIS cloud-typing algorithm) tend to show better agreement between MODIS and MISR cloud-top heights than most of the other cloud types. They generally have high optical thicknesses so both instrument retrievals should be able to obtain cloud-top height fairly accurately. The differences are distributed over a slightly larger range at SGP than CFARR. The mean difference was found to be −0.4 ± 1.5 km at SGP when both instrument retrievals located these clouds above 5 km and 0.5 ± 1.2 when they were found below 5 km. When both instrument retrievals detected these clouds at CFARR below 5 km (i.e., for the majority of these cases), the mean difference between MODIS and MISR cloud-top heights was 0.1 ± 1.1 km. There were a slightly larger number of pixels with both cloud-top heights above 5 km at SGP where clouds are in general at higher altitudes there.

4.3. Opaque ice clouds

Opaque ice clouds show a difference in MODIS-MISR cloud-top height between −5 and 5 km at SGP, but this range is slightly larger at CFARR. The peak is fairly well defined at SGP, but much broader at CFARR. Although the agreement is good between MODIS and MISR cloud-top heights at SGP, both in term of where these clouds are with respect to the 5 km level and in terms of the average difference (−0.3 ± 1.5 km), there are some notable discrepancies at CFARR. First, there are a non-negligible number of pixels where MISR cloud-top heights are found below 5 km, which could indicate the presence of a lower cloud layer. Second, some of these cases also show MODIS cloud-top heights below 5 km, and this could be an indication that the cloud-typing algorithm has more difficulties in detecting cloud overlap at CFARR. However, clouds tend to be at a lower altitude at CFARR than at SGP, so they can be fully glaciated but with a cloud-top height close to 5 km. Without external information, we can only hypothesize that some overlap situations may not be detected with the PH0405 cloud-typing algorithm. Perhaps the contrast exhibited by the optically thick ice cloud is somehow less than the contrast exhibited by a low-level cloud. Situations where MISR cloud-top heights do not exceed 5 km constitute 25% of all opaque ice cloud pixels at CFARR, but 13% at SGP.

4.4. Cirrus clouds

Cirrus clouds show a binomial distribution of the difference in cloud-top heights at both sites. At SGP, we find that 67% of all cirrus pixels have both MODIS and MISR cloud-top heights above 5 km and within −1.2 ± 2.3 km of each other on average. These pixels seem to be populating the largest of the two maxima. The secondary maximum occurs for differences of between 5–6 km and indicate that MODIS cloud-top heights are much higher than for MISR. About 21% of all cirrus cloud pixels have MODIS cloud-top heights above 5 km and MISR cloud-top height below 5 km. For these pixels, the average difference between MODIS and MISR cloud-top heights is 6.3 ± 2.3 km. At CFARR, the percentage of cirrus cloud pixels with both retrievals above 5 km was 30% with an average difference of −1.9 ± 2.7 km. Compared with what is found at SGP, this represents a much smaller fraction of all cirrus pixels. In addition, 23% of all cirrus pixels at CFARR had MODIS cloud-top heights above 5 km and MISR below 5 km. This suggests that at both sites, roughly 20% of the cirrus pixels could contain cloud overlap that was undetected by the cloud-typing method. Pavolonis and Heidinger (2004) found that if the low-level water cloud is optically thin or broken, the cloud-typing algorithm may not detect the overlap, and would indicate a cirrus cloud instead. Another explanation could be that errors in surface height delineation in MISR stereo height associated with a bad wind correction could lead to false low-level cloud detections. While at SGP, cirrus cloud pixels with MODIS cloud-top heights below 5 km amounted to 12%, at CFARR this number is about 47%. Since it was found that cloud layers are more often broken at CFARR than SGP (Naud et al., 2005a), it is possible that cirrus cloud pixels at CFARR could contain cloud overlap even if PH0405 does not discriminate it. Assuming this is the case, it is also possible that the MODIS cloud-top height algorithm only detects the lowest cloud layer as would MISR stereo heights. Without independent retrievals of separate cloud layer optical thicknesses, this hypothesis can not be verified here.

4.5. Overlap

The differences in CTH for the overlap cloud type in Fig. 3a, b also show a binomial distribution. The largest maximum is found around 0 km at both sites with a large spread. The second maximum is found at about 6 km at SGP and 4–5 km at CFARR. Cloud overlap pixels with MODIS cloud-top heights above 5 km and MISR cloud-top heights below 5 km were found for 26% of all cloud overlap pixels at SGP and for 40% of all overlap pixels at CFARR. Pixels with both MODIS and MISR retrievals above 5 km were found for 61% of all overlap pixels at SGP and 30% of all pixels at CFARR. There seems to be a greater probability for MISR to detect cirrus clouds in overlap situations at SGP than CFARR, either because the high clouds at SGP exhibit a greater contrast or that the water clouds at SGP exhibit a smaller contrast than at CFARR.

The radar data from CFARR and SGP for all of 2000 and 2001 were used to determine the distribution of differences in cloud-top heights between the highest and lowest cloud layers when more than one cloud layer is present (Fig. 4). This figure provides a benchmark to evaluate if the differences between MODIS and MISR CTH values behave in a similar manner as radar retrievals when more than one cloud layer is present. The "+" symbols show the contribution to the distribution of situations where the highest cloud layer had a cloud-top height greater than 5 km and the lowest layer had a cloud-top height of less than 5 km.

Fig. 4 shows how differences at CFARR are less than 2 km for a majority of cases, with equally probable separations between 2 and 6 km, and a sharp decrease to a zero frequency of occurrence at 10 km. When the difference in cloud-top heights was greater than 4 km, the highest cloud layer was always above 5 km whilst the lowest layer was below 5 km. For differences in cloud-top height less than 4 km, the two cloud layers can both be present above 5 km or both below 5 km. When we divided the tropopause into three regions limited by 4 km and 7 km altitudes, instead of the two regions limited by the 5 km altitude, the frequency of occurrence of both layers being present in the same altitude range (i.e. 0–4 km, 4–7 km or above 7 km regions) amounts to nearly 50% of all multilayer situations (compared to about 25% at SGP). With the results shown in Fig. 3b, the distribution of the difference in MODIS-MISR cloud-top height when cloud overlap is detected seems to follow the distribution of radar layer separation.

For SGP, there are two maxima for cloud layer separations obtained with the radar data (Fig. 4), one in accordance with CFARR at about 4 km and another for separations of about 8–9 km (at SGP clouds can attain altitudes up to 15 km). Situations where the two cloud layers are present on a different side of the 5 km altitude level account for all cases that constitute the cloud-

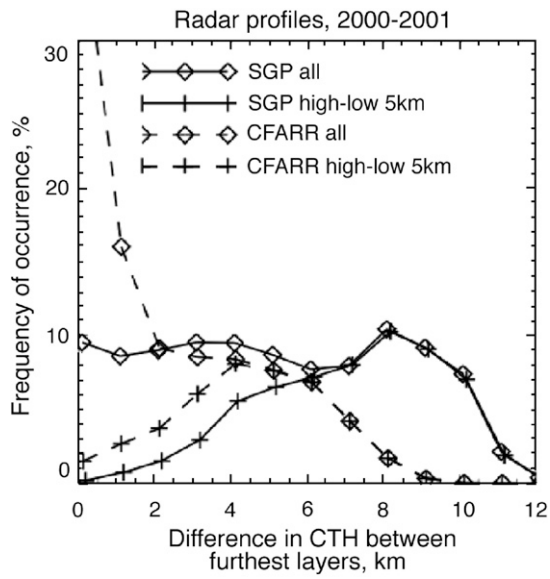

Fig. 4. Frequency of occurrence of the difference of cloud-top height between highest cloud layer and lowest cloud layer when more than one layer were present over CFARR and SGP radars during 2000 and 2001. The diamond symbols represent all cases, whereas the + symbols only show the contribution from situation where the highest layer has its top above 5 km and the lowest below 5 km.

top separations beyond the second maximum at 7 km, and for most of the cases with differences greater than 4 km. On Fig. 3a, the secondary maximum for the difference in cloud-top heights greater than 5 km was found to be smaller. This could come from inaccuracies in MODIS cloud-top heights as clouds are higher and optically thinner, causing an underestimate in the cloud-top height of the highest cloud layer in the scene and thus a smaller difference in cloud-top height with MISR.

5. Conclusions

MODIS and MISR cloud-top heights were derived and compared for 54 scenes over the SGP and CFARR millimeter cloud radar sites to assess if their CTH differences could help in cloud overlap detection. The differences were compared with radar and with results obtained from a cloud-typing method applied to MODIS data and developed by Pavolonis and Heidinger (2004) and Pavolonis et al. (2005).

Once all the scenes without radar data and with single-layered clouds were excluded, we found larger differences between MODIS and MISR cloud-top heights in cloud overlap situations. However, the differences were not always large when the radar data was used to identify multilayer situations. For some situations, both instruments gave very good retrievals of the cloud-top height of the highest layer. For other cases, MODIS and MISR tended to miss the highest cloud layer and were both assigned to the top of the lowest cloud layer. Thus the main conclusion from the radar comparison is that large differences between MODIS and MISR cloud-top heights were not systematically found when more than one cloud layer was present.

To increase the number of points of comparison, we used a cloud-typing method applied to MODIS data (Pavolonis & Heidinger, 2004; Pavolonis et al., 2005) that can discriminate situations where thin cirrus overlaps a water cloud. We found that large differences between MODIS and MISR cloud-top heights occurred predominantly for pixels either showing a cloud overlap type or a cirrus cloud type. We suggest that the latter cases were in fact overlap situations that could not be detected with PH0405, but we do not exclude the possibility that they could also be caused by errors in MISR cloud-top heights such as surface pixel contamination, the level of highest contrast being closer to cloud base than top, differences in resolution and different geolocation alignment between both instruments in broken cloud situations. For the other cloud types, the two retrievals were in fairly good agreement.

When cloud-typing or radar detected more than one cloud layer, we found a large number of occurrences where MISR cloud-top heights could detect the highest cloud layer, so the difference between MODIS and MISR cloud-top heights alone can only help for cloud overlap detection in about 30–40% of all situations detected with PH0405. However, the radar comparison also hinted that this method could be used when clouds of the same phase overlap. In addition, the difference method could also help to understand those situations where the cloud-typing algorithm gives “cirrus” as the cloud type when it should give “overlap”.

It would be important to use lidar measurements of cloud optical thickness profiles to understand situations that cause MISR cloud-top heights to succeed in detecting a high cloud layer even if a lower cloud is present and to assess how often MISR stereo height can be trusted in overlap situations. The recent launch of CloudSat (Stephens et al., 2002) and CALIPSO (Winker et al., 2003) will provide new tools to assess the merits of the passive estimate of cloud-top heights.

Acknowledgments

This research was sponsored in part by NASA Radiation Sciences and Terra-Aqua Data Analysis Programs, DOE/ARM and by the Earth Science Enterprise. C. Naud thanks the NASA Goddard Institute for Space Studies for their institutional support. MISR stereo data were obtained from the NASA Langley Research Center Atmospheric Sciences DAAC and MODIS Level 1 data were obtained from the Goddard Earth Sciences DAAC. The CFARR data were obtained through the CLOUDMAP2 consortium from the Council for the Central Laboratory of the Research Councils (CCLRC) and the authors would like to thank Elizabeth Slack (RAL) and Eugene Clothiaux (PSU) for the processing and access. The SGP-ARM data were obtained from the ARM archive (http://www.archive.arm.gov). The authors specifically acknowledge the support and encouragement of Dr. A. Del Genio of GISS, Prof. J.-P. Muller of UCL, Dr. David Diner of JPL and Dr. Hal Maring of the NASA Radiation Program at NASA headquarters. In addition, the authors are grateful to three anonymous reviewers for their comments. The views, opinions, and findings contained in this report are those of the authors and should

not be construed as an official National Oceanic and Atmospheric Administration or U.S. Government position, policy, or decision.

References

Baum, B. A., Frey, R. A., Mace, G. G., Harkey, M. K., & Yang, P. (2003). Nighttime multilayer cloud detection using MODIS and ARM data. *Journal of Applied Meteorology*, *42*, 905−919.

Baum, B. A., & Spinhirne, J. D. (2000). Remote sensing of cloud properties using MODIS airborne simulator imagery during SUCCESS. 3. Cloud overlap. *Journal of Geophysical Research*, *105*, 11,793−11,804.

Baum, B. A., Uttal, T., Poellot, M., Ackerman, T. P., Alavarez, J. M., Intrieri, J., et al. (1995). Satellite remote sensing of multiple cloud layers. *Journal of Atmospheric Sciences*, *52*(23), 4210−4230.

Chang, F. -L., & Li, Z. (2005). A new method for detection of cirrus overlapping water clouds and determination of their optical properties. *Journal of Atmospheric Sciences*, *62*, 3993−4009.

Clothiaux, E. E., Ackermann, T. P., Mace, G. C., Moran, K. P., Marchand, R. T., Miller, M. A., et al. (2000). Objective determination of cloud-top heights and radar reflectivities using a combination of active remote sensors at the ARM CART sites. *Journal of Applied Meteorology*, *39*, 645−665.

Diner, D. J., Beckert, J. C., Reilly, T. H., Bruegge, C. J., Conel, J. E., Kahn, R. A., et al. (1998). Multi-angle Imaging SpectroRadiometer (MISR) Instrument description and experiment overview. *IEEE Transactions on Geoscience and Remote Sensing*, *36*, 1072−1087.

Hahn, C. J., & Warren, S. G. (2002). *Cloud climatology for land stations worldwide, 1971–1996.* Numerical Data Package NDP-026D Oak Ridge, TN: Carbon Dioxide Information Analysis Center 35 pp.

Hahn, C. J., Warren, S. G., Lonon, J., Chervin, R. M., & Jenne, R. (1982). *Atlas of simultaneous occurrence of different cloud types over the ocean. NCAR Tech. Note TN-201+STR.* 212 pp. [NTIS PB83-152074].

Hahn, C. J., Warren, S. G., Lonon, J., Chervin, R. M., & Jenne, R. (1984). *Atlas of simultaneous occurrence of different cloud types over land. NCAR Tech. Note TN-241+STR.* 214 pp.

Heidinger, A. K., & Pavolonis, M. J. (2005). Global daytime distribution of overlapping cloud from NOAA's Advanced Very High Resolution Radiometer. *Journal of Climate*, *18*(22), 4772−4784.

Ho, S., Lin, B., Minnis, P., & Fan, T. (2003). Estimates of cloud vertical structure and water amount over tropical oceans using VIRS and TMI data. *Journal of Geophysical Research*, *108*, 4419. doi:10.1029/2002JD003298

Huang, J., Minnis, P., Lin, B., Yi, Y., Khaiyer, M. M., Arduini, R. F., et al. (2005). Advanced retrievals of multilayered cloud properties using multispectral measurements. *Journal of Geophysical Research*, *110*, D15S18. doi:10.1029/2004JD005101

Mace, G. G., Zhang, Y., Platnick, S., King, M. D., Minnis, P., & Yang, P. (2005). Evaluation of cirrus cloud properties derived from MODIS data using cloud properties derived from ground-based observations collected at the ARM SGP site. *Journal of Applied Meteorology*, *44*, 221−240.

Marchand, R. T., Ackerman, T. P., & Moroney, C. M. (in press). An assessment of Multi-Angle Imaging SpectroRadiometer (MISR) stereo-derived cloud top heights and cloud top winds using ground-based radar, lidar and microwave radiometer. *Journal of Geophysical Research*.

Menzel, W. P., Baum, B., Strabala, K., & Frey, R. (2002). *Cloud-top properties and cloud phase algorithm theoretical basis document. ATBD_MOD_04.* NASA Goddard Space Flight Center (Available on http://modis-atmos.gsfc.nasa.gov/MOD06_L2/atbd.html)

Menzel, W. P., Smith, W. L., & Stewart, T. R. (1983). Improved cloud motion wind vector and height assignment using VAS. *Journal of Climate and Applied Meteorology*, *22*, 377−384.

Moroney, C., Davies, R., & Muller, J. -P. (2002). Operational retrieval of cloud-top heights using MISR data. *IEEE Transactions on Geoscience and Remote Sensing*, *40*, 1532−1540.

Muller, J. -P., Mandanayake, A., Moroney, C., Davies, R., Diner, D. J., & Paradise, S. (2002). MISR stereoscopic image matchers: Techniques and results. *IEEE Transactions on Geoscience and Remote Sensing*, *40*, 1547−1559.

Nasiri, S., & Baum, B. A. (2004). Daytime multilayered cloud detection using multispectral imager data. *Journal of Atmospheric and Oceanic Technology*, *21*, 1145−1155.

Naud, C., Muller, J. -P., & Clothiaux, E. E. (2002). Comparison of cloud top heights derived from MISR stereo and MODIS CO_2-slicing. *Geophysical Research Letters*, *29*. doi:10.1029/2002GL015460

Naud, C., Muller, J. -P., Clothiaux, E. E., Baum, B. A., & Menzel, W. P. (2005). Intercomparison of multiple years of MODIS, MISR and radar cloud-top heights. *Annals of Geophysics*, *23*, 2415−2424.

Naud, C., Muller, J. -P., & de Valk, P. (2005). On the use of ICESat-GLAS measurements for MODIS and SEVIRI cloud-top height accuracy assessment. *Geophysical Research Letters*, *32*, L19815. doi:10.1029/2005GL023275

Pavolonis, M. J., & Heidinger, A. K. (2004). Daytime cloud overlap detection from AVHRR and VIIRS. *Journal of Applied Meteorology*, *43*(5), 762−778.

Pavolonis, M. J., Heidinger, A. K., & Uttal, T. (2005). Daytime global cloud typing from AVHRR and VIIRS: Algorithm description, validation, and comparisons. *Journal of Applied Meteorology*, *44*, 804−826.

Salomonson, V. V., Barnes, W. L., Maymon, P. W., Montgomery, H. E., & Ostrow, H. (1989). MODIS: Advanced facility instrument for studies of the earth as a system. *IEEE Transactions on Geoscience and Remote Sensing*, *27*, 145−153.

Stephens, G. L. & coauthors (2002). The CloudSat mission and the A-Train: A new dimension of space-based observations of clouds and precipitation. *Bulletin of the American Meteorological Society*, *83*, 1771−1790.

Winker, D. M., Pelon, J., & McCormick, M. P. (2003). The CALIPSO mission: Spaceborne lidar for observation of aerosols and clouds. *Proceedings of SPIE, the International Society for Optical Engineering*, *4893*, 1−11.